Fibre-Optic Photoacoustic Beacon and 2D Sparse Sensor Array for 3D Tracking of Needles

Christian Baker*, Weidong Liang*, Richard Colchester†, Peng Lei‡, Francois Joubert*, Sebastien Ourselin*, Simeon West§, Athanasios Diamantopoulos¶, Adrien Desjardins†, Wenfeng Xia*

* *King's College London*, London, U.K., † *University College London*, London, U.K., ‡ *GBA Institute of Collaborative Innovation*, Guangzhou, China., § *University College London Hospital*, London, U.K., ¶ *St Thomas' Hospital*, London, U.K.

***Abstract*—Accurate knowledge of the needle tip location during percutaneous procedures such as liver and breast biopsies, cancer treatment, drug delivery, and fetal blood transfusion would reduce adverse events, misdiagnoses and failed procedures. We have developed a novel trackable ultrasonic needle and 3D tracking system for such percutaneous medical needle procedures. The location of the needle tip is annotated onto the anatomical ultrasound images being used to guide the procedure, with the quantitative distance of the needle tip from the ultrasound imaging plane also visualised. The device works by transmitting pulses of ultrasound from our proprietary low-cost fibre-optic trackable needle which are detected by a sparse sensor array located on the patient's skin. This novel solution allows truly simultaneous 3D tracking and imaging with any ultrasound or other imaging system, in contrast to existing ultrasonic solutions which either provide only 2D tracking or must reduce the imaging frame rate to avoid interference. Tracking accuracy was assessed in water to depths of 14 cm and up to 3 cm from the ultrasound imaging plane: the spatial-average bias between tracked and true positions was 0.37 mm and the spatial-average repeatability was 1.2 mm.**

***Index Terms*—Needle tracking, real-time, fibre-optic ultrasound, minimally-invasive surgery**

I. Introduction

Real-time imaging is often used to guide the percutaneous insertion of a medical needle to its target: for example, it is common to use hand-held ultrasound (US) imaging to guide solid organ (i.e. liver, kidney) biopsies [1] and percutaneous ablation therapeutic procedures for cancer treatment [2]. However, localisation of the needle tip is often difficult due to specular reflections from the needle shaft [3, 4], tissue heterogeneity [5] or uncertainty about the elevational location of the needle tip; due to the 2D nature of the US guidance imagery, misalignment and of the needle shaft and imaging plane, often due to needle bending, can obscure the position of the needle tip. Accurate and precise knowledge of the true location of the needle tip in 3D would therefore reduce the likelihood of adverse events and failed procedures: for liver biopsy, 30% of procedures must be repeated, the false-positive rate is 7%, and up to 5% result in heavy bleeding and 1% in hospitalisation [6]. Outcomes are highly dependent on the clinicians' skills, who resort to costly MRI or X-ray for the most difficult insertions; clinicians report a desired maximum placement error of 2 mm while encountering errors of up to 5 mm [7].

Active needle tip tracking—where electromagnetic or ultrasonic signals are detected or generated by transducers integrated into the needle tip—has the potential to provide clinicians with accurate real-time knowledge of the location of the tip even when obscured in the guidance image. Existing methods include needle-integration of: electromagnetic (EM) sensors [8]; piezoelectric US sensors [9] and transmitters [10]; fibre-optic US sensors [11–13] and transmitters [14]; and fibre-optic photoacoustic generation [15]. For EM tracking, the needle tip sensor is localised via detection of the gradient of a known EM field to which it is exposed. While this method can provide 3D localisation, it is sensitive to EM disturbances from ferromagnetic material in the surgical environment, requires a bulky EM field generator close to the surgical site, and has a tracking resolution that can exceed 3 mm [16]. Ultrasonic methods can provide sub-millimetre tracking accuracy, typically via an embedded piezoelectric transmitter or receiver. Two limitations have impeded clinical deployment: reliance on research US platforms with poor image quality [11, 12]; and the necessity to interleave tracking and imaging frames for the avoidance of interference, reducing frame rates. Recent works have utilised miniature fibre-optic hydrophones (FOHs) to detect transmission from the US imaging array being used for guidance [11–13], avoiding interference. We previously demonstrated a 2D FOH tracking system that works as an adjunct to a commercial US imaging system, using the imaging pulse sequence for tracking and therefore allowing truly simultaneous imaging and tracking [13]. However, tracking was 2D, limited to locations within the imaging plane. Similar piezoelectric methods have been demonstrated [9].

Needle insertion procedures are guided using linear- or curvilinear-arrays (i.e. 2D US imaging), therefore the use of a needle-integrated US sensor for 3D tracking requires either additional transmitting arrays to be added to the US probe, as in [11] and a patented tracking system from University College London [17], or derivation of the elevational position of the needle tip from the 2D pulse sequences. In [9] and [13], it is shown that it is possible to provide a qualitative visualisation of the elevational distance of the needle tip from the imaging

This work was supported by the Beijing Institute of Collaborative Innovation.

plane using the amplitude of the received signals, but the sensitivity of this method is likely to be spatially dependent and affected by the distribution of tissues in the imaging plane. [18] presents a machine-learning based method for estimating the distance of the needle tip from the imaging plane, but it has only been tested in homogenous media, and it was found that the signal-to-noise ratios were too poor for tracking further than approximately 6 mm from the imaging plane.

Needle-integrated fibre-optic US transmitters (FOTs) are well-suited to 3D tracking. They are small enough to be easily needle-integrated, especially in comparison to piezoelectric transmitters and their associated electronics. Transmitted US pulses can be detected by the imaging array or a dedicated tracking array; receiving arrays are more simple and cost effective that transmitting systems. In this configuration, 3D localisation can be performed using a single US pulse transmission. FOTs exploit the photoacoustic (PA) effect to generate US via laser-illumination of optically-absorbent material deposited at the fibre tip [19]. Recent fibre-optic transmitter coatings have comprised Polydimethylsiloxane (PDMS), which is biocompatible and has a high thermal expansion coefficient, in combination with high optical absorption materials such as carbon nanotubes (CNT) [20], candle soot nanoparticles (CNP) [21] and reduced graphene oxide (rGO) [22].

Tracking of a needle-integrated PDMS-CNT FOT was demonstrated in [14]. A research US system was used to acquire interleaved tracking and imaging frames from a linear array US transducer with a bandwidth of 5 MHz to 14 MHz. Imaging frame rate was low, tracking was not real-time, and due to the reliance on a 1D linear array, tracking was only possible in 2D. Accuracy was only assessed up to a depth of 50 mm

This paper describes a new 3D US needle tracking system based on a needle-integrated FOT and 2D sparse tracking array, and which is therefore independent of the imaging system being used for guidance. The FOT was designed to reduce interference with US imaging. The accuracy of the system was assessed in water to depths of 14 cm and up to 3 cm from the US imaging plane.

II. Tracking System

A. Overview

The tracking system comprises two acoustic components: the needle with integrated US transmitter (the "trackable needle"), and the extracorporeal US receiver array (the "tracking array"). The current implementation of the tracking array was designed to be mounted to an Edan C5-1Q curvilinear array (Edan Instruments, Shenzhen, China), and the tracking system was configured to operate in conjunction with an Edan AX8 imaging system (Edan Instruments, Shenzhen, China). The trackable needle and tracking array are connected to a tracking console (see Figure 1) which comprises: a 532 nm, 50 µJ, fibre-coupled pulsed laser (Changchun New Industries Optoelectronics Technology Co., Ltd, Changchun, China) for generating photoacoustic US transmissions from the trackable needle tip; an arbitrary waveform generator (M2p.6560-x4, Spectrum Instrumentation GmbH, Grosshansdorf, Germany) for triggering the laser; a multichannel digital acquisition card (DN2 Digitizer Netbox, Spectrum Instrumentation GmbH, Grosshansdorf, Germany) for acquisition of signals from the tracking array; a frame grabber (ProCapture HDMI, Nanjing Magewell Electronics Co., Ltd, Nanjing, China) for acquisition of guidance images from the US imaging system; and a PC running a desktop application which displays acquired guidance images annotated with tracking information.

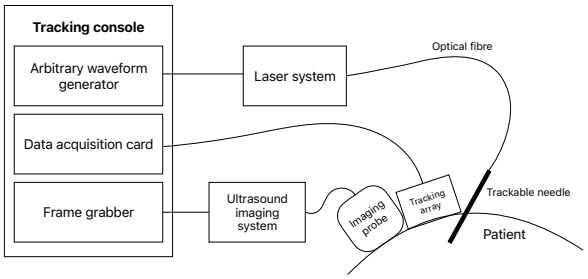

Fig. 1. Schematic diagram of the 3D US needle tracking system connected to the US imaging system.

US transmissions from the trackable needle are detected by the tracking array, and processed in order to determine the 3D location of the needle tip relative to the tracking array. This coordinate is then transformed to a position relative to the imaging probe, and then finally to a pixel within the acquired guidance image and a distance from the imaging plane.

B. Trackable Needle

The trackable needle is 10 cm long, 18-gauge and bevel-tipped; it is intended to replace the stylet of a 15 cm long coaxial needle biopsy system such as the TEMNO Evolution Biopsy Device (Merit Medical, Utah, USA). A fibre-optic US transmitter is fixed into the lumen of the needle, epoxied within the needle hub and needle bevel. The transmitter comprises a 200 µm core (254 µm outer diameter) optical fibre (FG200-LEP, Thorlabs, New Jersey, USA) which has been dip-coated in a composite of PDMS (MED1000, Avantor, Pennsylvania, USA) and rGO (Sigma-Aldrich, Massachusetts, USA). This composite was chosen, as in [22], because of its ready availability compared to CNP and its improved biocompatibility compared to CNT. The PDMS-rGO composite was prepared as in [20]. The fibre tips were dip-coated by hand until a nominally spherical coating with a diameter of approximately twice that of the fibre was adhered to the cleaved face. The rGO concentration was chosen empirically to be as low as possible while still completely absorbing the light transmitted through the fibre: a weight-weight ratio of 4% rGO to unthinned PDMS provided absorption spread throughout the coating, which was approximately 500 µm in diameter, as shown in Figure 2. The coated fibres were left to cure for 24 hours with the coated face pointing vertically downwards.

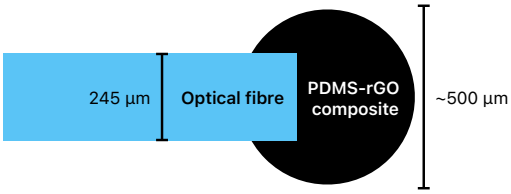

Fig. 2. Cross-sectional diagram of the tip of a fibre-optic US transmitter.

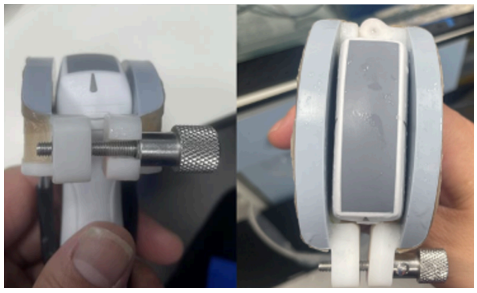

Fig. 3. The 16 element tracking array mounted to the Edan C51-Q imaging probe.

C. Tracking Array

A bespoke 16 element tracking array was manufactured by Eintik Technologies Co., Ltd. (Shanghai, China) to fit the Edan C5-1Q imaging probe, comprising 8 evenly-distributed elements either side of the imaging plane, as shown in Figure 3. The centre frequency of the square, 1×1 mm piezoelectric elements was 1 MHz.

D. Tracking Software and Algorithm

A Windows 11 desktop application (Python 3.12) triggered the generation of US from the trackable needle and acquired the resulting signals from the tracking array. The tracking rate was 15 Hz, with each tracked position generated from 30 tracking pulses (1 kHz pulse rate) by averaging the received waveforms. The envelopes of the 16 average waveforms were detected as described in [13], and the signal-to-noise ratio (SNR) was estimated. Low SNR waveforms (SNR <5) were discarded. In the remaining waveforms, the time-of-arrival (ToA) of the tracking pulse at each array element was measured, relative to the time at which the tracking pulse was generated. The waveform SNR associated with each ToA was used as a relative confidence metric. Iterative multilateration (Gauss-Newton least-squares iterative optimizer) was used to determine the needle position from the ToAs. If the optimizer failed to converge, then the ToA with the lowest confidence was removed from the set, and the multilateration repeated.

The resulting 3D coordinate relative to the tracking array was then registered to the imaging probe's coordinate system by applying a transformation matrix derived from comparison of the apparent location of the needle tip in high contrast, low-artefact US images to corresponding tracked locations. The transformed 3D coordinate was then corrected for spatially-variant tracking bias, determined using the accuracy assessment methodology described below. The corrected 3D coordinate was converted to a pixel within the most recently acquired US imaging frame using knowledge of the geometry of the US imaging frames. The tracked location was then visualised on this pixel as a cross-hair. A colour map was applied to the cross-hair to indicate the distance of the needle tip from the imaging plane.

III. Accuracy Assessment Methodology

The accuracy of the tracking system was assessed in a tank of water by moving the trackable needle tip to known locations relative to the imaging probe using a 3-axis motion control system (1N150 linear stages, Thorlabs, NJ, USA). The imaging and tracking array assembly was attached to a fixed mount with its face submersed in the water tank, pointing vertically downwards. The position grid covered the right-hand side of the US imaging field of view (15 cm imaging depth). Accuracy was assessed in 4 axial-lateral planes 0 cm, 1 cm, 2 cm and 3 cm from the imaging plane respectively. At each location, 30 measurements of the tracked position were made. The first accuracy scan found a spatially-variant bias between tracked and true out-of-plane positions. This bias was characterised using radial basis function interpolation and stored to disk so that it could be corrected for as part of the software's tracking pipeline. A second scan was then completed with each axial-lateral plane having a resolution of 20 mm.

IV. Results

Figure 4 shows the tracking repeatability, determined by taking the vector magnitude of the standard deviations of the repeat measurements of tracked position. In plane, the spatial average repeatability was ±0.98 mm, and over the whole volume assessed it was ±1.2 mm. Bias was less than 0.5 mm on average across the whole volume, which is believed to be within the uncertainty of the alignment and measurement procedure.

V. Conclusion

This paper has demonstrated that a new prototype US needle tracking system based on a needle-integrated fibre-optic transmitter and sparse extracorporeal sensor array is capable of 3D tracking of a needle tip in water with an accuracy suitable for solid-organ biopsy procedures, for which placement error of no more than 2 mm is desired [7]. However, sound-speed heterogeneity and attenuation in tissue may detrimentally affect accuracy, and the effect of interference with US imaging has not yet been assessed. Future work will include phantom and *ex vivo* tissue experiments to determine the suitability of the technology for clinical use.

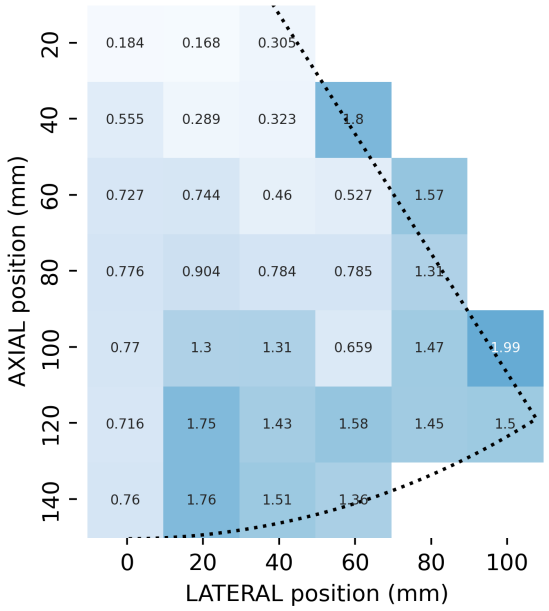

Fig. 4. The repeatability (magnitude of the standard deviation of 30 repeat measurements) of tracked position, in millimetres, in the imaging plane. The dashed line indicates the extent of the field of view of the US imaging system.

References

[1] L. Buscarini *et al.*, "Ultrasound-guided fine-needle biopsy of focal liver lesions: Techniques, diagnostic accuracy and complications," *Journal of Hepatology*, vol. 11, no. 3, pp. 344–348, Nov. 1990.

[2] J. W. Kim *et al.*, "Ultrasound-guided percutaneous radiofrequency ablation of liver tumors: How we do it safely and completely," *Korean Journal of Radiology*, vol. 16, no. 6, p. 1226, 2015.

[3] K. Nichols *et al.*, "Changes in ultrasonographic echogenicity and visibility of needles with changes in angles of insonation," *Journal of Vascular and Interventional Radiology*, vol. 14, no. 12, pp. 1553–1557, Dec. 2003.

[4] V. Uppal *et al.*, "Effect of beam steering on the visibility of echogenic and non-echogenic needles: A laboratory study," *Canadian Journal of Anesthesia/Journal canadien d'anesthésie*, vol. 61, no. 10, pp. 909–915, Jul. 2014.

[5] G. Reusz *et al.*, "Needle-related ultrasound artifacts and their importance in anaesthetic practice," *British Journal of Anaesthesia*, vol. 112, no. 5, pp. 794–802, May 2014.

[6] A. Khalifa *et al.*, "The utility of liver biopsy in 2020," *Current Opinion in Gastroenterology*, vol. 36, no. 3, pp. 184–191, May 2020.

[7] T. L. de Jong *et al.*, "Needle placement errors: Do we need steerable needles in interventional radiology?" *Medical Devices: Evidence and Research*, vol. Volume 11, pp. 259–265, Aug. 2018.

[8] A. Hakime *et al.*, "Electromagnetic-tracked biopsy under ultrasound guidance: Preliminary results," *Cardiovasc Intervent Radiol*, vol. 35, no. 4, pp. 898–905, Aug. 2012.

[9] T. Kåsine *et al.*, "Needle tip tracking for ultrasound-guided peripheral nerve block procedures—an observer blinded, randomised, controlled, crossover study on a phantom model," *Acta Anaesthesiologica Scandinavica*, vol. 63, no. 8, pp. 1055–1062, Apr. 2019.

[10] J. J. Langberg *et al.*, "The echo-transponder electrode catheter: A new method for mapping the left ventricle," *J Am Coll Cardiol*, vol. 12, no. 1, pp. 218–223, Jul. 1988.

[11] W. Xia *et al.*, "Looking beyond the imaging plane: 3d needle tracking with a linear array ultrasound probe," *Sci Rep*, vol. 7, no. 1, Jun. 2017.

[12] S. J. Mathews *et al.*, "Ultrasonic needle tracking with dynamic electronic focusing," *Ultrasound in Medicine & Biology*, vol. 48, no. 3, pp. 520–529, Mar. 2022.

[13] C. Baker *et al.*, "Intraoperative needle tip tracking with an integrated fibre-optic ultrasound sensor," *Sensors*, vol. 22, no. 23, p. 9035, Nov. 2022.

[14] W. Xia *et al.*, "Ultrasonic needle tracking with a fibre-optic ultrasound transmitter for guidance of minimally invasive fetal surgery," in *Lecture Notes in Computer Science*, Springer International Publishing, 2017, pp. 637–645.

[15] M. A. Lediju Bell *et al.*, "Photoacoustic-based visual servoing of a needle tip," *Scientific Reports*, vol. 8, no. 1, Oct. 2018.

[16] P. Beigi *et al.*, "Enhancement of needle visualization and localization in ultrasound," *Int J Comput Assist Radiol Surg*, vol. 16, no. 1, pp. 169–178, Sep. 2020.

[17] A. Desjardins, "A method and apparatus for determining the location of a medical instrument with respect to ultrasound imaging, and a medical instrument to facilitate such determination," WO2014174305A3, 2013.

[18] A. Arjas *et al.*, "Neural network kalman filtering for 3-d object tracking from linear array ultrasound data," *IEEE Transactions on Ultrasonics, Ferroelectrics, and Frequency Control*, vol. 69, no. 5, pp. 1691–1702, May 2022.

[19] W. Xia, Ed., *Biomedical Photoacoustics: Technology and Applications*. Springer Nature Switzerland, 2024.

[20] R. J. Colchester *et al.*, "Laser-generated ultrasound with optical fibres using functionalised carbon nanotube composite coatings," *Applied Physics Letters*, vol. 104, no. 17, Apr. 2014.

[21] W.-Y. Chang *et al.*, "Candle soot nanoparticles-polydimethylsiloxane composites for laser ultrasound transducers," *Applied Physics Letters*, vol. 107, no. 16, Oct. 2015.

[22] R. J. Colchester *et al.*, "A directional fibre optic ultrasound transmitter based on a reduced graphene oxide and polydimethylsiloxane composite," *Applied Physics Letters*, vol. 114, no. 11, Mar. 2019.